Determining the Refractive Properties of Microlenses in Stellest Glasses

Tuva Källberg
tuva.kallberg@gmail.com

under the direction of
Assoc. Prof. Linda Lundström
M.Sc. Charlie Börjeson
Department of Applied Physics
KTH Royal Institute of Technology

Research Academy for Young Scientists
July 14, 2021

Abstract

Myopia (near-sightedness) is a common visual defect affecting billions of people worldwide. Usually, symptoms of myopia can be easily corrected with negative lenses, however, the condition itself is hard to cure. Recently, novel lenses aiming to control myopia progression in children have been developed and made commercially available. One of these is the Stellest Glasses produced by Essilor, which have shown to slow the progression of myopia. The glasses consist of microlenses placed in eleven rings around the fovea which are designed to slow down the elongation of the eye. This study investigated the refractive properties of the lenses by using a wavefront sensor to obtain the Zernike coefficients for defocus and spherical aberration for the lenses. By constructing an optical system utilizing a laser beam passing through a single lens, the wavefront created by that lens could be magnified and then recreated using a telescope and a wavefront sensor. To determine the glasses' effect on the wearers vision another optical system was used that simultaneously measured the reflected wavefront in both the foveal and peripheral vision. The results show a slight difference in power between the microlenses and suggest that lenses in the far periphery are weaker than ones close to the fovea. Furthermore, the glasses appear to have an effect on the vision and reduced the relative peripheral refraction.

Acknowledgements

Primarily, I would like to show my gratitude towards my mentors Linda Lundström, and Charlie Börjeson, for their guidance through this research project and for helping me understand the complex concepts with which I was not previously familiar. The time I spent at AlbaNova was highly educational and memorable thanks to their supervision. I would also like to thank my project partner Shirley Lidman for amazing companionship and friendship which made these weeks at AlbaNova truly incredible.

I am especially thankful towards Rays - for Excellence, Kjell & Märta Beijers Stiftelse and Europaskolan, for giving me this opportunity to learn and grow as a person.

Furthermore, none of this would have been possible without the Rays organizers and I would therefore like to thank them for their hard work, support, and valuable feedback.

Contents

1 Introduction

Myopia (near-sightedness) is a visual defect affecting billions of people worldwide. It commonly starts developing in childhood and affects both the peripheral vision and the foveal vision. The foveal vision is the focus while the peripheral vision is everything seen to the side of the central focus. Myopia has become a major problem, and The World Health Organisation estimates the number of myopic people to rise to 5 billion people by 2050 [1]. Preventing the progression of myopia is a work in progress and recently glasses containing microlenses have proven to be effective [2]. This study focused on the Stellest glasses produced by Essilor that have been reported to slow the progression of myopia in children with more than 60%. The glasses consist of microlenses placed in eleven rings in the periphery. [3]

1.1 Theory

In order to comprehend the principles of detection of optical aberrations with wavefront sensing, an introduction to the field will be given. Concepts such as the optics of lenses, and function of a wavefront sensor and telescope are explained in the following section.

1.1.1 The Human Eye

The eye consists of four major optical components, the cornea, the pupil, the lens, and the retina, see Figure 1. The pupil is located approximately 3 mm behind the cornea and limits the amount of light entering the eye. The lens directly behind the pupil focuses the incoming light onto the retina, forming an image [4]. An emmetropic eye focuses the light directly onto the retina, creating a sharp image [1].

The far point of the eye is defined as the location of the object a relaxed eye focuses onto the retina. For an emmetropic eye, the far point will be at infinity, since parallel light then enters the eye. To image an object closer than the far point, muscles around the lens will contract resulting in a thicker lens with a shorter focal length, allowing the

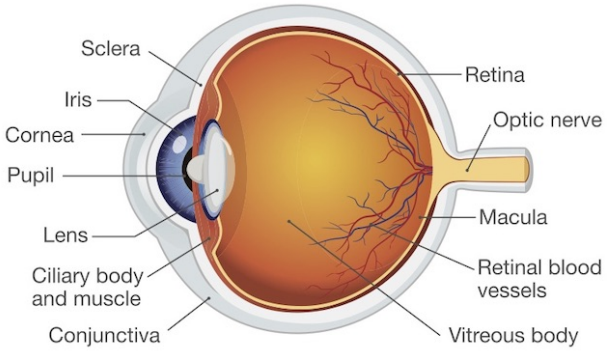

Figure 1: The anatomy of the human eye [5].

lens to properly focus the image onto the retina. [4]

Refractive errors such as myopia and hyperopia (far-sightedness) occur when a relaxed eye cannot focus light from infinity directly onto the retina. A myopic eye focuses the light at a point in front of the retina, while a hyperopic eye focuses it at a point behind the retina, see Figure 2 [1]. The far point for a relaxed myopic eye is at a finite distance from the eye. A myopic eye can only accommodate for objects closer than the far point, meaning that objects further away will not be imaged sharply onto the retina. A hyperopic eye, however, will always have to accommodate. [4]

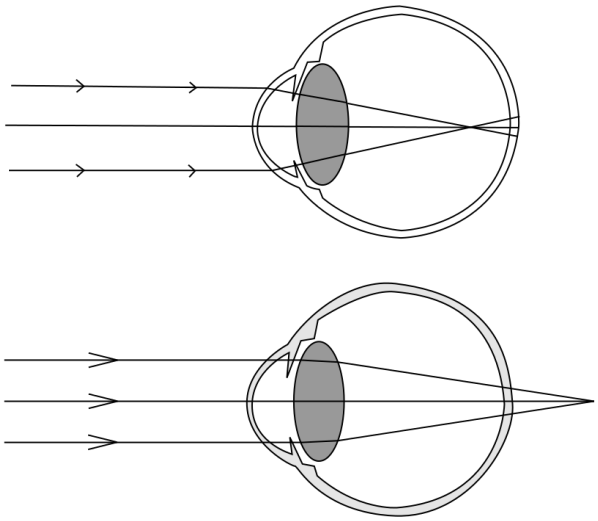

Figure 2: Focal length for myopic and hyperopic eye [6].

1.1.2 Lenses

A lens is a refracting device that changes the wavefront of rays passing through it. The reconfiguration of the light differs depending on the shape of the lens. Generally, there are two different categories of lenses, positive lenses, and negative lenses. Positive lenses are convex. Parallel rays entering the lens will converge to a point, the focal point. The distance from the middle of the lens to the focal point is called the focal length, see Figure 3. Negative lenses are concave. Rays entering a negative lens diverge. When parallel light enters a negative lens the rays appear to diverge from a point behind the lens. The focal length for a negative lens is the distance between this point and the center of the lens, see Figure 3. [7]

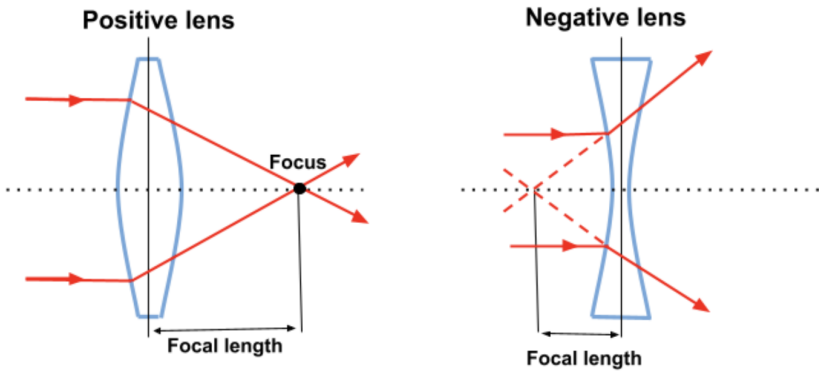

Figure 3: Focal length for positive and negative lenses.

Unlike a spherical lens, an aspherical lens does not have a surface profile matching that of a sphere or a cylinder. Typically, an aspherical lens reduces spherical aberration while spherical lenses generally cause spherical aberration. [8]

How much a lens refracts light passing through it determines the power of the lens. The power corresponds to the focal length of the lens - a shorter focal length amounts to a stronger lens [9]. A common unit for the power of a lens is diopters (D) which is defined by Equation (1) [10], where f is the focal length in meters, and P is the lens power in diopters.

$$\mathrm{P} = \frac{1}{f}, \tag{1}$$

1.1.3 Aberrations

A lens can have various imperfections in its ability to image an object - these are called aberrations. Defocus is a common aberration in the human eye and is the cause of both myopia and hyperopia. The aberration entails that the focal point for an optical system is shifted away from the desired focal point. [4]

Spherical aberration occurs when parallel rays are focused onto different points on the optical axis, as shown in Figure 4. Peripheral rays passing through the edge of the pupil are focused differently than rays passing through the center. [11]

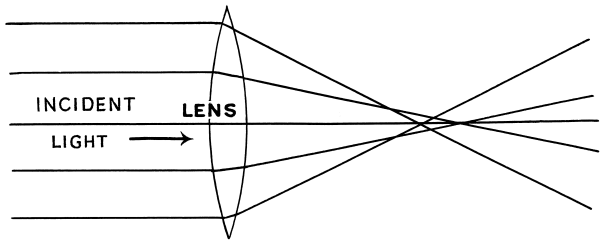

Figure 4: Illustration of a lens with spherical aberration where rays entering the edge of the lens are focused in a different point that ones entering the center [12].

1.1.4 Wavefront Sensor

The power and aberrations of lenses in an optical system affect the direction of the rays emerging from it, thus giving the rays a specific wavefront. A wavefront sensor can recreate an image of the wavefront and thereby capture information about the power and aberrations in the optical system. Parallel rays have a flat wavefront while a point source of light has a spherical wavefront. [4]

The Hartmann-Shack Wavefront Sensor (HSWS) is the most common type of ocular wavefront sensor. It consists of an array of small lenses called lenslets, that focus the light on a detector that is placed on the focal plane of the lenslets as shown in Figure 5. If the wavefront is tilted, the focal point from that lenslet will be shifted from its optical axis. By analyzing the shifts of the focal points of the lenslets, the wavefront can be reconstructed. [4]

The displacement of each spot from the flat reference wavefront spot represents the local slope of the aberrated wavefront over the pupil. From these slopes, the wavefront can be described with Zernike coefficients calculated by the program for the wavefront sensor. [1]

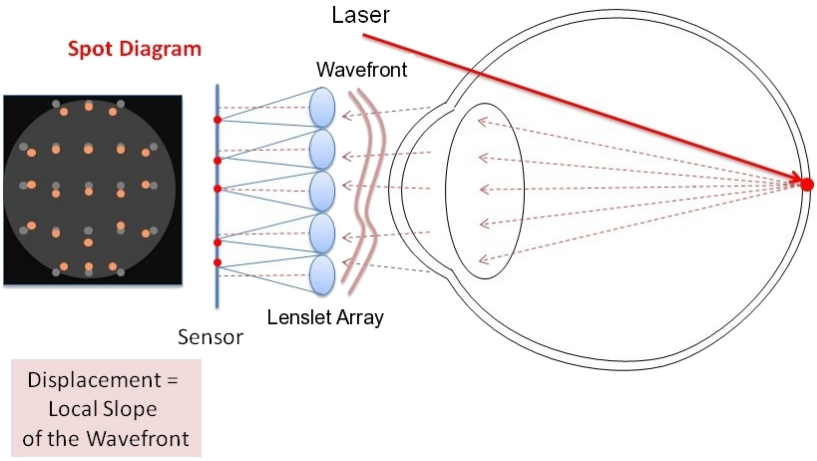

Figure 5: Principle of the Hartmann-Shack Wavefront Sensor [13].

1.1.5 Zernike Polynomials

The Zernike polynomials form an orthogonal basis on the unit disk and can, thus, be used to mathematically describe the shape of the wavefront. The shape of the wavefront can be extracted with the coefficients for each Zernike polynomial. As each aberration has its own Zernike polynomial, a coefficient for each aberration can be calculated by the wavefront sensor program. The Zernike coefficient for defocus is described in Figure 6, where a flat wavefront is compared to one with defocus. The Zernike coefficient for defocus is the difference in height, (Z_d in Figure 6) for a wavefront with defocus compared to a flat wavefront. This difference is indicated in µm. [1]

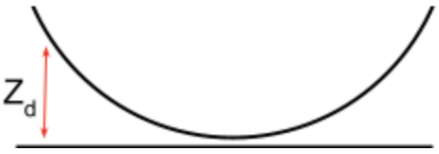

Figure 6: Defocus compared to a plane wavefront.

1.1.6 Telescope

The wavefront sensor cannot be placed directly in front of the eye. Therefore the wavefront from the eye or lens needs to be reconstructed, which is done with a telescope.

A 4f Keplerian telescope uses two positive lenses to magnify a wavefront [4]. The magnification of the telescope can be calculated with Equation (2), in which h_1 is the height of the wavefront, i.e the diameter of the lens the light passes through, that is being magnified, h_2 is the height of the magnified image, f_1 is the focal length of the first lens and f_2 is the focal length of the second lens. [4]

$$M_\alpha = \frac{h_1}{h_2} = \frac{f_1}{f_2} \tag{2}$$

The first lens in a 4f Keplerian telescope is placed at its focal length (f_1) away from the object that is being magnified. The second lens is at a distance of $f_1 + f_2$ away from the first lens, and lastly, the wavefront sensor is f_2 away from the second lens, see Figure 7, giving the telescope a total length of 4f, which is the reason behind its name. [4]

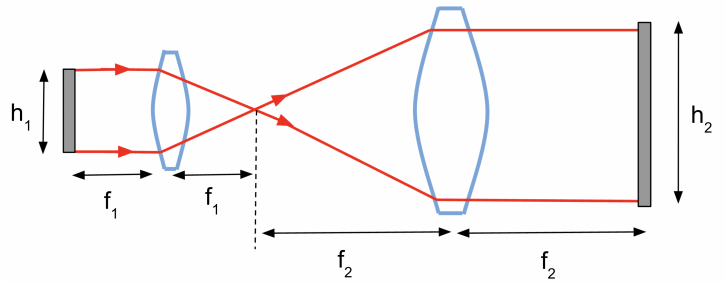

Figure 7: Principle of a 4f Keplerian telescope, where the height of the first lens (h_1) is magnified to the height of the second lens (h_2).

1.1.7 Dual-Angle Open Field Wavefront Sensor

The dual-angle open field wavefront sensor captures the Zernike coefficients for foveal and peripheral aberrations and is primarily used for researching myopia. Simultaneous measurements of horizontal visual field angles of 20°, of the same eye, are done with the sensor. Each of the two channels seen in Figure 8 consists of a Hartmann-Shack wavefront sensor, a 2 lens telescope, beam splitters, and a laser. The system also consists of a hot mirror that reflects infra-red light. [14]

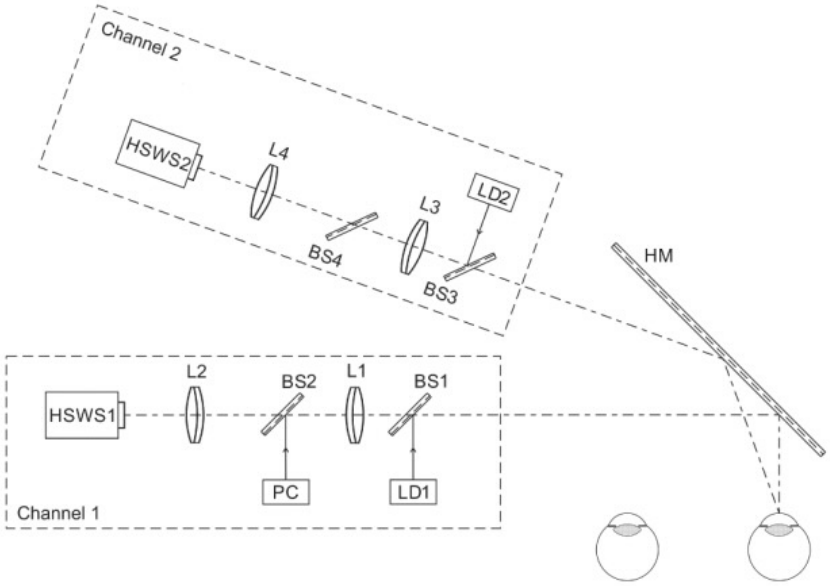

Figure 8: The construction of the Dual-Angle Open Field Wavefront Sensor where L1, L2, L3 and L4 are the lenses, BS1, BS2, BS3 and BS4 are the beam splitters, and HM is the hot mirror.[14]

1.1.8 Stellest Glasses by Essilor

Microlenses have shown to be effective in reducing the progression of myopia. However, the reasons behind this beneficial effect are not fully understood.[2] A new type of microlens glasses, called the Stellest glasses were launched in 2020 by the company Essilor. During clinical trials on children, the glasses showed a more than 60% slowdown in myopia progression, compared to children wearing glasses with single vision lenses. H.A.L.T (Highly Aspherical Lenslet Target) technology is used in the Stellest glasses, which con-

sist of eleven rings with aspherical microlenses, as shown in Figure 9. [3] Generally the main glass in the Stellest glasses holds refractive power to correct myopia, however, the glass in this study holds no refractive power as it makes it easier to only measure the refractive power of the microlenses.

The patent application for the Stellest glasses, made by Essilor, state that the refractive properties of the microlenses from different rings might change according to a gaussian or quadratic function [15].

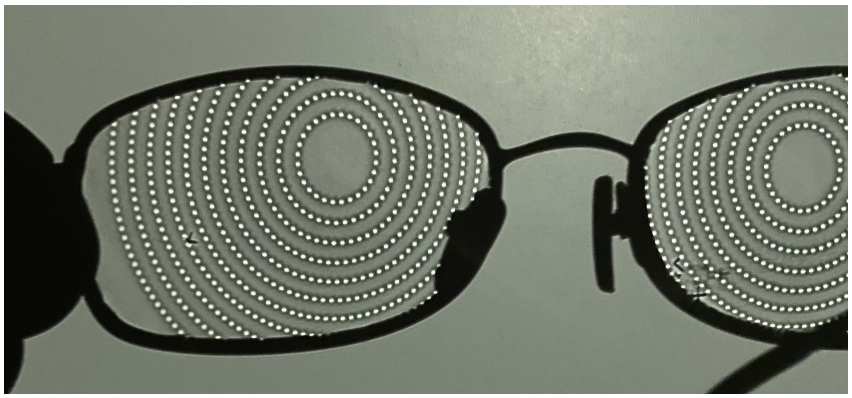

Figure 9: Shadow of Stellest glasses showing the eleven rings of microlenses.

1.1.9 Analysis of Variance

The ANOVA (Analysis of Variance) method assesses the relative size of variance between groups compared to the average variance within groups. An ANOVA test calculates an F-statistic value and a p-value. The F-value is defined as variation between sample means, divided by, variation within the samples. A large F-value implies that means of the groups are different from each other compared to the variation of the individual observations in each group [16]. A p-value is a measure of the probability that an observed difference could have occurred by random chance. The lower the p-value, the greater the statistical significance of the observed difference. [17]

1.2 Aim of the Study

The aim of this study was to examine the properties of the microlenses in the Stellest glasses by Essilor. Only limited information about the design of the glasses has been revealed and details about the refractive properties of the glasses are therefore unknown. Understanding the construction of the glasses and how they shape the light was the primary goal of the project as this information could contribute to clarifying how the glasses help control myopia progression. Knowing this is a crucial part of being able to slow down the development of myopia in children. Specifically, the intention of the study was to determine if all the micro-lenses have the same power and exhibit the same spherical aberration and if not determine how these properties vary from each other depending on the lens position on the glasses and their angle from the pupil.

2 Method

The method used to examine the construction of the glasses and their effect on the sight was divided into two main parts. First, the refractive properties of the microlenses in the glasses were determined, secondly, their effect on the vision of the wearer was investigated.

2.1 Measurement of Refractive Properties of Microlenses

Determining the refractive properties of the microlenses can be divided into preparation, measurement, and analysis of data.

2.1.1 Alignment of Reference Light

First, the reference light was aligned to ensure the alignment of the laser beam with one axis. Two polarising filters were put in front of the laser to lower its intensity. The laser was aligned onto one axis with an alignment disk of frosted glass and a screen placed behind it. It was to pass through the center hole of the alignment disk when the disk and screen were placed as seen in figure 10. Thereafter, the alignment disk and screen were

moved back and the laser was aligned to pass through the hole. The process was repeated until the laser beam passed through the hole at all distances without adjustments, thus signaling proper alignment.

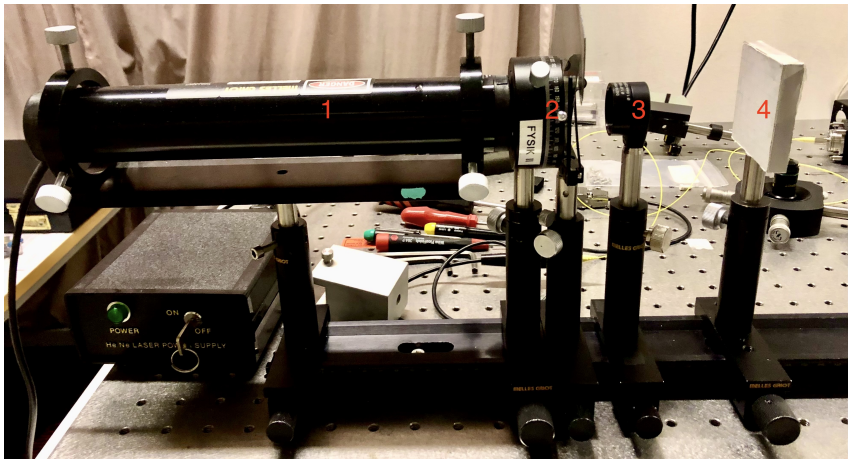

Figure 10: Setup for aligning the laser with alignment disk and screen close to the laser. The figure shows an alignment disk (3), and screen (4), placed behind the polarising filters (2), which lower the intensity of the laser (1).

A microscope was aligned to focus the laser onto a specific point. The microscope, attached to a microscope holder, was placed in a mount clamped to the optical rail, ensuring alignment to the same axis. The height of the microscope was adjusted such that the spot of the laser was centered on the alignment disk which was placed behind the microscope. Thereafter, a pinhole was placed in the focus point of the microscope. Light going through the pinhole comes out cone-shaped. To make the light parallel a positive +10D lens was placed 100 mm behind the pinhole.

Four different methods were used to find the correct placement of the lens. The first method was to measure the diameter of the spot the laser made on the screen when it was placed behind the lens. An aperture was placed behind the lens to give the spot on the screen sharp edges. The placement of the lens was slightly altered until the size of the spot on the screen was consistent regardless of the screen's distance from the lens. For the other method, a handheld telescope was used. The telescope was focused on a spot far away outside, which represented a spot in infinity. Without changing the focus of the telescope, it was placed in a mount on the optical rail, see Figure 11. The placement

of the lens was slightly altered while simultaneously looking at the pinhole through the telescope to find the sharpest image of the pinhole.

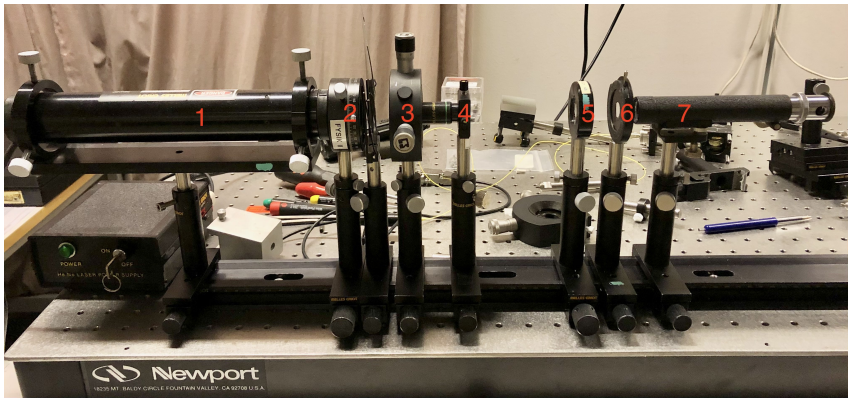

Figure 11: Setup for using the handheld telescope to verify that the light exiting the lens was parallel. The figure shows the microscope (3), placed behind the polarizing filters (2), and the pinhole (4), placed at the focus point of the microscope. The lens (5) is placed behind the pinhole, followed by an aperture (6), and the hand-held telescope (7).

Thirdly, a shear plate was placed behind the lens and the aperture. When the laser was turned on, red lines were shown on the shear plate. The lens was adjusted until the lines on the shear plate were horizontal. Lastly, the Hartmann-Shack wavefront Sensor was placed behind the lens which showed the wavefront of the light. The lens was adjusted until the wavefront was flat i.e the Zernike coefficient for defocus was 0.

2.1.2 Installing Stand for Glasses

Attaching the glasses to the optical rail was done with a filter holder with two screws, with rubber ends. The glasses were placed behind an aperture that in turn was placed behind the first lens. When the placement of the glasses had been determined they were removed from the filter holder. A small piece of black paper with a hole with a diameter of 1 mm was put in the filter holder.

2.1.3 Alignment of Telescope

The image of the wavefront, originally of size 1.1 mm, was magnified by a factor of 3.5, determined by Equation (2). The power of the lenses in diopters was calculated to the

lenses' focal length in millimeters with Equation (1). The lenses used for the telescope were positive, one +7.1 D (140 mm) lens and one +20 D (50 mm) lens.

A 4f Keplerian telescope was aligned. The lens with a focal length of 50 mm was placed 50 mm from the glasses, the placement was controlled with the handheld telescope. The second lens with a focal length of 140 mm was placed 190 mm from the first lens. The placement of this lens was controlled with the shear plate and the wavefront sensor.

Lastly, the wavefront sensor was put into position. Ensuring the correct placement of the sensor was done by putting strong lenses behind the small black paper. The position of the wavefront sensor was altered until the lens had no effect on the registered pupil size on the sensor.

2.1.4 Measurements

A reference picture of the aberrations in the optical system without glasses was taken and the values for these aberrations were removed from the aberration values collected from the measurements of the glasses. The glasses were mounted horizontally in the filter holder, placed in position for the laser to hit the optical center of the left glass i.e the part without microlenses. The registered pupil size on the wavefront sensor was set to 2.742 mm. In order for the laser to hit a microlens in the first circle on the nasal side, the glasses were moved horizontally to the left. The Zernike coefficients for defocus and spherical aberration were recorded. The same process was repeated for one lens in each circle on the nasal side of the center. This was repeated three times without alterations made to the optical system. Measurements were done the same way on the temporal side. The positions of the microlenses were determined by measuring each lens distance from the optical center. The distance from the pupil to the optical center of the glasses was also measured.

2.1.5 Analysis of Data

The lenses were numbered 1-18, 1 being the lens closest to the edge on the temporal side and 18 being the one closest to the edge on the nasal side. This was combined with the position of the lens as well as the lens angle from the pupil. The angle was calculated using the tangent function for right-angled triangles. The data was then plotted and a polynomial regression were made. An ANOVA test was used to determine the statistical significance of the result by obtaining an F-statistic value and a p-value. The standard deviation for the measurements on each lens was calculate and a mean of the standard deviations were determined.

2.2 Evaluation of Stellest Glasses Influence on Human Vision

The dual angle system was used to measure the glasses' general influence on the vision of a user. First, the laser was set to approximately 0.033 mW. Subject 1 sat in the system without the Stellest glasses and looked at two crosses on a screen 60 cm from the eye. The measurement was started when the subject's pupils were in the right position i.e reflecting the light onto the center of the wavefront sensors, and then stopped after 30 seconds. Three measurements were done on each subject without glasses and then three with glasses. No changes in the optical system were made between the measurements.

2.2.1 Analysis of Data

The Zernike coefficients collected during the measurements were used to calculate the relative peripheral refraction of each measurement. The values were plotted for each subject and a linear regression was made.

3 Results

The first part of the results includes the results of the measurements for the properties of the microlenses, while the second part contains the measurements of the glasses' influence

on human vision.

3.1 Properties of Microlenses

The values of the Zernike coefficients for defocus from measurements on the temporal and the nasal side of the glasses found in Appendix A are combined in Figure 12. The graph of the Zernike coefficients for spherical aberration based on values in Appendix B are shown in Figure 13.

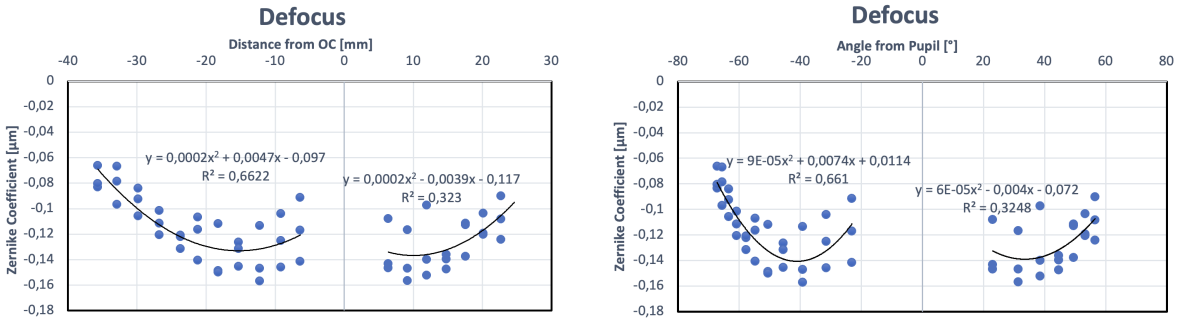

(a) The Zernike coefficient for defocus variation depending on the lens distance from the optical center in millimeters.

(b) The Zernike coefficient for defocus variation depending on the lens angle from the pupil in degrees

Figure 12: The Zernike coefficients for defocus. Regression of a quadratic formula was made for the temporal side and nasal side. The R^2 value represents the goodness-of-fit.

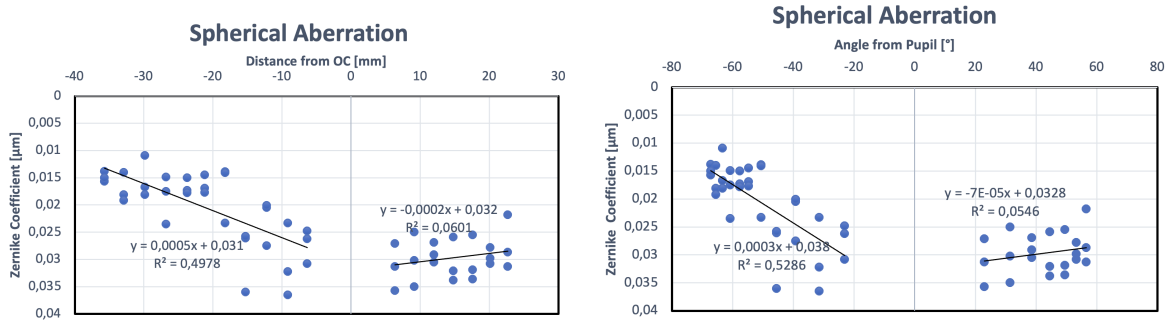

(a) The Zernike coefficient for spherical aberration variation depending on the lens distance from the optical center in millimeters.

(b) The Zernike coefficient for spherical aberration variation depending on the lens angle from the pupil.

Figure 13: The Zernike coefficients for spherical aberration. Linear regression was made for the temporal side and nasal side. The R^2 value represents the goodness-of-fit.

Table 1 shows the standard deviation mean of the standard deviation for the measurements of each lens found in Appendix C.

Table 1: The standard deviation means for the Zernike coefficients of each lens, for defocus and spherical aberration.

	Standard deviation mean
Defocus	0.012976883
Spherical aberration	0.003006456

Calculations done with an ANOVA test gave F-statistic values and p-values based on values found in Appendix D. The results for both defocus and spherical aberration are shown in Table 2.

Table 2: Values collected from ANOVA test for Zernike coefficients for defocus and spherical aberration.

Aberration	**F-statistic value**	**P-value**
Defocus	3.76821	0.0004
Spherical Aberration	7.87623	$<$0.0001

3.2 The Glasses Influence on Human Vision

The influence of the Stellest glasses on human vision is shown in Figure 14 and 15. For subject one wearing glasses, two out of three measurements shows a larger relative peripheral refraction than without, see Figure 14, indicating a smaller refractive error with glasses. For subject two, see Figure 15, three out of three measurements show a larger relative peripheral refraction with glasses. The values used to calculate the relative peripheral refraction are found in Appendix E.

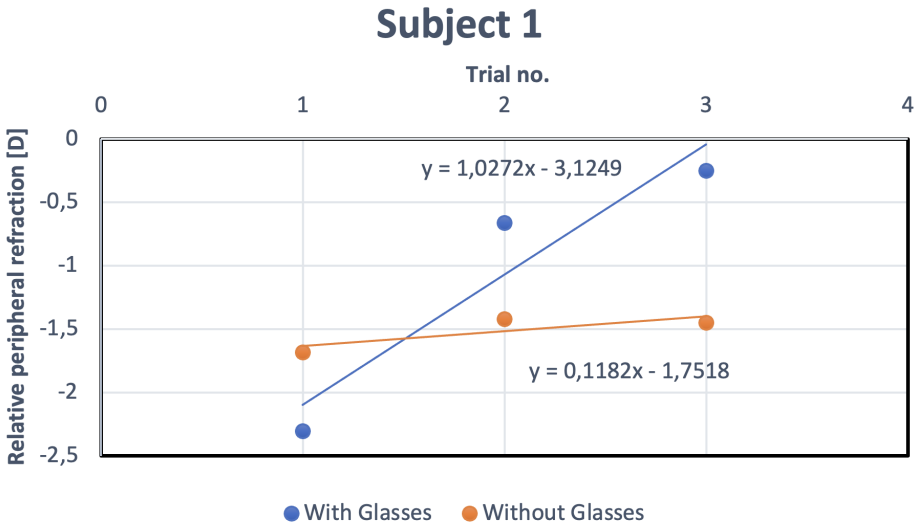

Figure 14: Relative peripheral refraction for subject 1, with and without glasses.

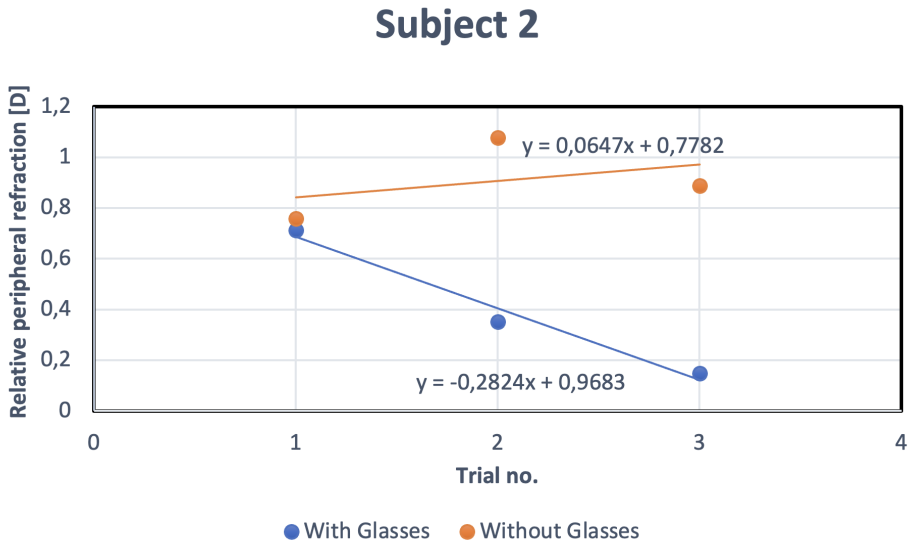

Figure 15: Relative peripheral refraction for subject 2, with and without glasses.

4 Discussion

The first subsection of the discussion consider the results for the properties of the microlenses, while the second part consider the glasses influence on the vision. Possible further studies are also discussed.

4.1 Refractive Properties of the Microlenses

For the purpose of determining the refractive properties of the microlenses in the Stellest glasses, this study provides evidence for a difference in refractive power between the microlenses in different rings. The study suggests that the Zernike coefficients for defocus approach zero for lenses further out in the periphery, see Figure 12a, indicating that lenses in the periphery are weaker than the ones close to the fovea. The Zernike coefficients for both the temporal side and the nasal side of the optical center appear to follow a quadratic function. This is credible as the alternative of them following a quadratic function was mentioned in the patent application for the glasses. However, the measurements lack precision. Although the quadratic function was the best fit for the values, the R^2 value for the temporal side as well as the nasal side is low implying that the quadratic function does not fit well. This is also supported by the high standard deviation mean for defocus.

The quadratic regression for the temporal side matches the data better than for the nasal side. The values of the Zernike coefficients in the far periphery are more precise than ones close to the fovea, which could be why the values of the temporal side have less diffusion. This is especially true when looking at Figure 12b, where the angle of the lens from the pupil is considered.

When looking at the values for spherical aberration there is no clear correlation between the size of the Zernike coefficient and the lens position on the glass. The precision of the values for each lens is weak, especially for the nasal side. This is also supported by the low R^2 value. A linear function of the values of the Zernike coefficients for spherical aberration can be suspected on the temporal side of the optic center, as the spread is slightly lower. But it is still hard to draw a conclusion regarding the microlenses spherical aberration due to imprecise measurements.

Both the values for defocus and spherical aberration have a low p-value suggesting that there is a clear difference between the values for microlenses from different rings, implying that the refractive properties of the lenses are in fact different.

4.2 Glasses Effect on Human Vision.

The results show that the relative peripheral refraction in diopters is closer to zero when the subjects are wearing the glasses than without. This indicates a smaller difference in refractive error between the fovea and periphery when wearing the glasses. However, the measurements without glasses appear more precise than ones with glasses, which could be a result of small differences in how the eye is placed relative to the microlenses. If the microlenses are moved slightly over the pupil the wavefront changes dramatically. The values suggest a difference in relative peripheral refraction, but no conclusions draws should be considered certain, due to the small quantity of data collected.

4.3 Further Studies

It would be useful for future studies to further investigate the construction and refractive properties of the glasses by measuring other Zernike coefficients for the microlenses. For this it might be necessary to improve the optical system built in this study, to better fit measurements of other Zernike coefficients. For measuring astigmatism it needs to be assured that the laser beam hits the lens straight from the front which requires altering the optical system used in this study. Measuring each individual lens might also be useful to determine how the refractive properties of the lenses vary between and/or within circles.

Based on the results in this study, future studies could also investigate how the refractive properties of the microlenses help decrease the progression of myopia in children. Understanding that would facilitate improving the technique for further treatment of myopia.

4.4 Conclusion

This study has found a slight difference in power between the microlenses. The lenses with a greater angle from the pupil seem to be weaker than ones close to the fovea. However, there was a large variation in the values which makes it difficult to draw strong conclusions

regarding the refractive properties of the microlenses. There are also indications that the glasses have an impact on human vision, but due to a lack of data, no certain conclusions may be drawn.

References

[1] Papadogiannis P. Myopia control and peripheral vision. KTH Royal Institute of Technology; 2021.

[2] Dickinson F. The Value of Micro-Lenses in Progressive Myopia. Clinical and Experimental Optometry. 1957;40(8):356–365.

[3] Essilor. Essilor's game-changing Stellest™ lens shown to slow down myopia progression in children by more than 60%. 2020.

[4] Börjeson C. Design of a compact wavefront sensor for measurements on the human eye; 2020.

[5] Image: "Eye Anatomy";. Available from: https://www.cvpdaytoneyedoctors.com/comprehensive-eye-exam/eye-anatomy/.

[6] Image: "Hypermetropia and Myopia";. Available from: https://commons.wikimedia.org/wiki/File:Hypermetropia_and_Myopia.svg.

[7] Hecht E. Optics 3rd ed., Eddison Wesley Longman; 1998.

[8] Kweon GI, Kim CH. Aspherical lens design by using a numerical analysis. Journal of the Korean Physical Society. 2007;51(1):93–103.

[9] Unsbo P. Optik1 Geometrisk och fysikalisk optik. 2021.

[10] SOBOTA S, SOBOTA M. Justerbar sökare till professionell filmkamera; 2012.

[11] Hecht E. Optics 3rd ed., Eddison Wesley Longman; 1998.

[12] Image: "Spherical aberration (PSF).";. Available from: https://commons.wikimedia.org/wiki/File:Spherical_aberration_(PSF).png.

[13] Image: "Shack hartmann";. Available from: https://commons.wikimedia.org/wiki/File:Shack_hartmann.jpg.

[14] Romashchenko D, Lundström L. Dual-angle open field wavefront sensor for simultaneous measurements of the central and peripheral human eye. Biomedical optics express. 2020;11(6):3125–3138.

[15] Guillot M GC. Lens element. 2018;(WO2019166657A1 (Patent)).

[16] Kim HY. Analysis of variance (ANOVA) comparing means of more than two groups. Restorative dentistry & endodontics. 2014;39(1):74–77.

[17] Thisted RA. What is a P-value. Departments of Statistics and Health Studies. 1998.

A Values of Zernike Coefficients for Defocus

Table 3: Values of Zernike coefficients for defocus trial 1.

Lens no.	Lens position	Lens angle	Zernike coefficient-Defocus
1	-140	-67.20153979	-0.0663
2	-129	-65.47886884	-0.0969
3	-117	-63.29949806	-0.1058
4	-105	-60.73200479	-0.1115
5	-93	-57.67623943	-0.1223
6	-83	-54.66374792	-0.1164
7	-71.5	-50.54482949	-0.1487
8	-60	-45.55625223	-0.1265
9	-48	-39.20365314	-0.1469
10	-36	-31.45682336	-0.1252
11	-25	-23.0175618	-0.1416
12	25	23.0175618	-0.1467
13	36	31.45682336	-0.1468
14	47	38.61411056	-0.1523
15	58	44.58509377	-0.1474
16	69	49.54103518	-0.1127
17	79	53.31801537	-0.1205
18	89	56.52761185	-0.1242

Table 4: Values of Zernike coefficients for defocus trial 2.

Lens no.	Lens position	Lens angle	Zernike coefficient-Defocus
1	-140	-67.20153979	-0.0833
2	-129	-65.47886884	-0.0786
3	-117	-63.29949806	-0.0840
4	-105	-60.73200479	-0.1206
5	-93	-57.67623943	-0.1210
6	-83	-54.66374792	-0.1069
7	-71.5	-50.54482949	-0.1120
8	-60	-45.55625223	-0.1315
9	-48	-39.20365314	-0.1133
10	-36	-31.45682336	-0.1459
11	-25	-23.0175618	-0.0914
12	25	23.0175618	-0.1433
13	36	31.45682336	-0.1566
14	47	38.61411056	-0.1400
15	58	44.58509377	-0.1396
16	69	49.54103518	-0.1376
17	79	53.31801537	-0.1194
18	89	56.52761185	-0.0901

Table 5: Values of Zernike coefficients for defocus trial 3.

Lens no.	Lens position	Lens angle	Zernike coefficient-Defocus
1	-140	-67.20153979	-0.0805
2	-129	-65.47886884	-0.0670
3	-117	-63.29949806	-0.0925
4	-105	-60.73200479	-0.1015
5	-93	-57.67623943	-0.1314
6	-83	-54.66374792	-0.1407
7	-71.5	-50.54482949	-0.1500
8	-60	-45.55625223	-0.1454
9	-48	-39.20365314	-0.1570
10	-36	-31.45682336	-0.1040
11	-25	-23.0175618	-0.1169
12	25	23.0175618	-0.1081
13	36	31.45682336	-0.1168
14	47	38.61411056	-0.0974
15	58	44.58509377	-0.1361
16	69	49.54103518	-0.1115
17	79	53.31801537	-0.1036
18	89	56.52761185	-0.1082

B Values of Zernike Coefficients for Spherical Aberration

Table 6: Values of Zernike coefficients for spherical aberration trial 1.

Lens no.	Lens position	Lens angle	Zernike coefficient-Spherical Aberration
1	-140	-67.20153979	0.0138
2	-129	-65.47886884	0.0140
3	-117	-63.29949806	0.0109
4	-105	-60.73200479	0.0149
5	-93	-57.67623943	0.0173
6	-83	-54.66374792	0.0169
7	-71.5	-50.54482949	0.0139
8	-60	-45.55625223	0.0261
9	-48	-39.20365314	0.0205
10	-36	-31.45682336	0.0365
11	-25	-23.0175618	0.0308
12	25	23.0175618	0.0313
13	36	31.45682336	0.0350
14	47	38.61411056	0.0269
15	58	44.58509377	0.0321
16	69	49.54103518	0.0336
17	79	53.31801537	0.0308
18	89	56.52761185	-0.0287

Table 7: Values of Zernike coefficients for spherical aberration trial 2.

Lens no.	Lens position	Lens angle	Zernike coefficient-Spherical Aberration
1	-140	-67.20153979	0.0157
2	-129	-65.47886884	0.0181
3	-117	-63.29949806	0.0167
4	-105	-60.73200479	0.0175
5	-93	-57.67623943	0.0178
6	-83	-54.66374792	0.0177
7	-71.5	-50.54482949	0.0233
8	-60	-45.55625223	0.0258
9	-48	-39.20365314	0.0275
10	-36	-31.45682336	0.0233
11	-25	-23.0175618	0.0248
12	25	23.0175618	0.0271
13	36	31.45682336	0.0302
14	47	38.61411056	0.0305
15	58	44.58509377	0.0338
16	69	49.54103518	0.0319
17	79	53.31801537	0.0298
18	89	56.52761185	0.0313

Table 8: Values of Zernike coefficients for spherical aberration trial 3.

Lens no.	Lens position	Lens angle	Zernike coefficient-Spherical Aberration
1	-140	-67.20153979	0.0150
2	-129	-65.47886884	0.0192
3	-117	-63.29949806	0.0181
4	-105	-60.73200479	0.0235
5	-93	-57.67623943	0.0150
6	-83	-54.66374792	0.0145
7	-71.5	-50.54482949	0.0141
8	-60	-45.55625223	0.0360
9	-48	-39.20365314	0.0201
10	-36	-31.45682336	0.0322
11	-25	-23.0175618	0.0262
12	25	23.0175618	0.0357
13	36	31.45682336	0.0250
14	47	38.61411056	0.0291
15	58	44.58509377	0.0259
16	69	49.54103518	0.0255
17	79	53.31801537	0.0278
18	89	56.52761185	0.0218

C Standard Deviation Values

Table 9: Standard deviation of measurements of Zernike coefficients for defocus for each lens.

Lens no.	**Standard deviation**
1	0.00744
2	0.01230
3	0.00890
4	0.00780
5	0.00463
6	0.01423
7	0.01761
8	0.00799
9	0.01868
10	0.01710
11	0.02049
12	0.01745
13	0.01693
14	0.02352
15	0.00472
16	0.01203
17	0.00772
18	0.01393

Table 10: Standard deviation of measurements of Zernike coefficients for spherical aberration for each lens.

Lens no.	**Standard deviation**
1	0.0007846
2	0.0022376
3	0.0031169
4	0.0036012
5	0.0012193
6	0.0013597
7	0.0043848
8	0.0047392
9	0.0033980
10	0.0054969
11	0.0025630
12	0.0035113
13	0.0040836
14	0.0014817
15	0.0033951
16	0.0034874
17	0.0012472
18	0.0040086

D Values from ANOVA Test

Table 11: Values from ANOVA test for defocus.

Group	N	Mean	Std. Dev	Std. Error
1	3	-0.0767	0.0091	0.0053
2	3	-0.0808	0.0151	0.0087
3	3	-0.0941	0.011	0.0063
4	3	-0.1112	0.0096	0.0055
5	3	-0.1249	0.0057	0.0033
6	3	-0.1213	0.0174	0.0101
7	3	-0.1369	0.0216	0.0125
8	3	-0.1345	0.0098	0.0057
9	3	-0.1391	0.0229	0.0132
10	3	-0.1250	0.0210	0.0121
11	3	-0.1166	0.0251	0.0145
12	3	-0.1327	0.0214	0.0123
13	3	-0.1401	0.0207	0.0120
14	3	-0.1299	0.0288	0.0166
15	3	-0.1410	0.0058	0.0033
16	3	-0.1206	0.0147	0.0085
17	3	-0.1145	0.0095	0.0055
18	3	-0.1075	0.0171	0.0099

Table 12: Values from ANOVA test for Spherical aberration.

Group	**N**	**Mean**	**Std. Dev**	**Std. Error**
1	3	0.0148	0.0010	0.0006
2	3	0.0171	0.0027	0.0016
3	3	0.0152	0.0038	0.0022
4	3	0.0186	0.0044	0.0025
5	3	0.0167	0.0015	0.0009
6	3	0.0164	0.0017	0.0010
7	3	0.0171	0.0054	0.0031
8	3	0.0293	0.0058	0.0034
9	3	0.0227	0.0042	0.0024
10	3	0.0307	0.0067	0.0039
11	3	0.0273	0.0031	0.0018
12	3	0.0314	0.0043	0.0025
13	3	0.0301	0.0050	0.0029
14	3	0.0288	0.0018	0.0010
15	3	0.0306	0.0042	0.0024
16	3	0.0303	0.0043	0.0025
17	3	0.0295	0.0015	0.0009
18	3	0.0273	0.0049	0.0028

E Values for the Glasses Influence on Human Vision

Table 13: Values for subject 1 with glasses. RE stands for refractive error and RPR stands for relative peripheral refraction.

Trial	Pupil size [mm]	RE fovea [D]	RE periphery [D]	RPR [D]
1	1.75	-1.308033381	-3.551688278	-2.301896773
2	1.75	-1.444633392	-2.103831344	-0.6622827377
3	1.75	-1.425203424	-1.713706303	-0.2475294003

Table 14: Values for subject 1 without glasses. RE stands for refractive error and RPR stands for relative peripheral refraction.

Trial	Pupil size [mm]	RE fovea [D]	RE periphery [D]	RPR [D]
1	1.75	-1.259330649	-2.97666228	-1.682214084
2	1.75	-1.402105182	-2.792599609	-1.418100616
3	1.75	-1.302025375	-2.805210568	-1.445772159

Table 15: Values for subject 2 with glasses. RE stands for refractive error and RPR stands for relative peripheral refraction.

Trial	Pupil size [mm]	RE fovea [D]	RE periphery [D]	RPR [D]
1	1.75	-1.182087335	-0.4529591736	0.7123121
2	1.75	-1.130702522	-0.5998079858	0.3508853105
3	1.75	-1.349683358	-1.166378911	0.1475729787

Table 16: Values for subject 2 without glasses. RE stands for refractive error and RPR stands for relative peripheral refraction.

Trial	Pupil size	RE fovea	RE periphery	RPR
1	1,75	-1,807187496	-1,056387327	0,7577143013
2	1,75	-1,970380319	-0,926769431	1,077895069
3	1,75	-2,176185498	-1,268714965	0,8871103833